γ-ray spectroscopy of ^{140}La decay for nuclear forensics applications

A. Mattera,[1] S. Waniganeththi,[1] N. Cabanas,[2] E. A. McCutchan,[1] S. Zhu,[1,*] C. Morse,[1] M. P. Carpenter,[3] J. P. Greene,[3] C. Müller-Gatermann,[3] M. Jandel,[4] P. C. Bender,[4] V. Tripathi,[5] C. Wibisono,[5] S. Ajayi,[5] L. T. Baby,[5] S. Bhattacharya,[5] S. L. Tabor,[5] J. M. Allmond,[6] T. J. Gray,[6,7] and T. T. King[6]

[1]*National Nuclear Data Center, Brookhaven National Laboratory, Upton, New York 11973-5000, USA*
[2]*Department of Chemistry, The University of North Carolina at Chapel Hill, Chapel Hill, North Carolina 27516, USA*
[3]*Physics Division, Argonne National Laboratory, Argonne, Illinois 60439, USA*
[4]*Department of Physics and Applied Physics, University of Massachusetts Lowell, Lowell, Massachusetts 01854, USA*
[5]*Department of Physics, Florida State University, Tallahassee, Florida 32306, USA*
[6]*Physics Division, Oak Ridge National Laboratory, Oak Ridge, Tennessee 37831, USA*
[7]*Department of Physics and Astronomy, University of Tennessee, Knoxville, Tennessee 37966, USA*

(Received 14 May 2025; accepted 13 November 2025; published 22 December 2025)

^{140}La is an important isotope in nuclear forensics. It is typically paired with ^{140}Ba as a chronometer for dating nuclear events. In this work, we report the results of two measurements performed to fully characterize the decay scheme of ^{140}La. The experiments were performed using the Gammasphere array at Argonne National Laboratory and the CLARION2 array at Florida State University. Sources of ^{140}La were produced through neutron irradiation of natural lanthanum (99.9% ^{139}La) in the University of Massachusetts Lowell research reactor. We identify a total of 40 transitions, three of which were not previously reported. An angular correlation analysis was conducted confirming current literature J assignments and mixing ratios. By considering all data available in the literature, we provide new recommended values for the intensities of the strongest transitions commonly used in applications.

DOI: 10.1103/4g27-8l8x

I. INTRODUCTION

Nuclear forensics analysis aims to determine the origin and history of nuclear material through appropriate analytical techniques. Postdetonation analysis is among the most challenging tasks of nuclear forensics, where information regarding a nuclear event is inferred from the analysis of its debris. Mass $A = 140$ is prominently produced in fission of major actinides, with mass yields of about 4.5–6% in fission of ^{235}U induced by neutrons with energies ranging from thermal to 14 MeV [1]; and noble gas ^{140}Xe, a precursor of ^{140}La, is one of the most abundant fission products, as shown in Fig. 1. These characteristics, combined with its half-life [$T_{1/2}$ = 1.67858(21) d [2]] and strong, high-energy 1596 keV γ-ray transition, make ^{140}La valuable not only for nuclear forensics but also for applications in the nuclear industry, such as quantifying rodwise power distribution in reactor fuel [3].

The time elapsed since the nuclear event, or *zero time,* is one of the quantities of interest. The zero time can be estimated through an analysis of the relative abundances of ^{140}La and its parent, ^{140}Ba. Both isotopes are produced in the β^- decay chain of ^{140}Xe, which is a noble gas that can easily go airborne, allowing its daughters to be detected far from the production site. The inability to contain the parent noble gas allows for the detection of ^{140}La and ^{140}Ba even after underground testing. Furthermore, since neither naturally exists, detection of these nuclides can be directly linked to a nuclear event. The activation technique, i.e., the detection of the characteristic γ rays emitted in the decay of radionuclides, is the most common way to quantify ^{140}La and ^{140}Ba. This method was applied in 2010 when the International Monitoring System [4] detected ^{140}Ba and ^{140}La in atmospheric samples. Following a 24-h collection, it was proved that the zero time could be estimated to within one day of the event [5]. More recently, measurement of ^{140}La was also proposed as a novel method to estimate the content of uranium in samples following neutron activation analysis [6].

The activation technique relies heavily on a solid knowledge of the intensities of selected γ-ray transitions. A recent study by Pommé *et al.* [7] showed that neither the Evaluated Nuclear Structure Data File (ENSDF) [8] nor the Decay Data Evaluation Project (DDEP) [9] contains ^{140}La decay data that are sufficiently precise or accurate to predict the zero-time effectively. Both databases had a bias to underestimate the zero time by a day. These limitations could arise from inaccuracies in the evaluated γ-ray intensities, currently based on experiments performed in 1991 and earlier, and highlight the need for updated decay data in order to reliably use ^{140}La in nuclear forensics.

^{140}La decays exclusively to ^{140}Ce ($\%\beta^- = 100$), with a $\beta^- Q$-value of 3762.2 (13) keV [10] and a half-life of 40.284 (3) h [2]. Direct decay from the $J^\pi = 3^-$ ground state of ^{140}La to the even-even ^{140}Ce ground state is highly forbidden, leading to the preferential population of excited states in the β^- decay process.

*Deceased.

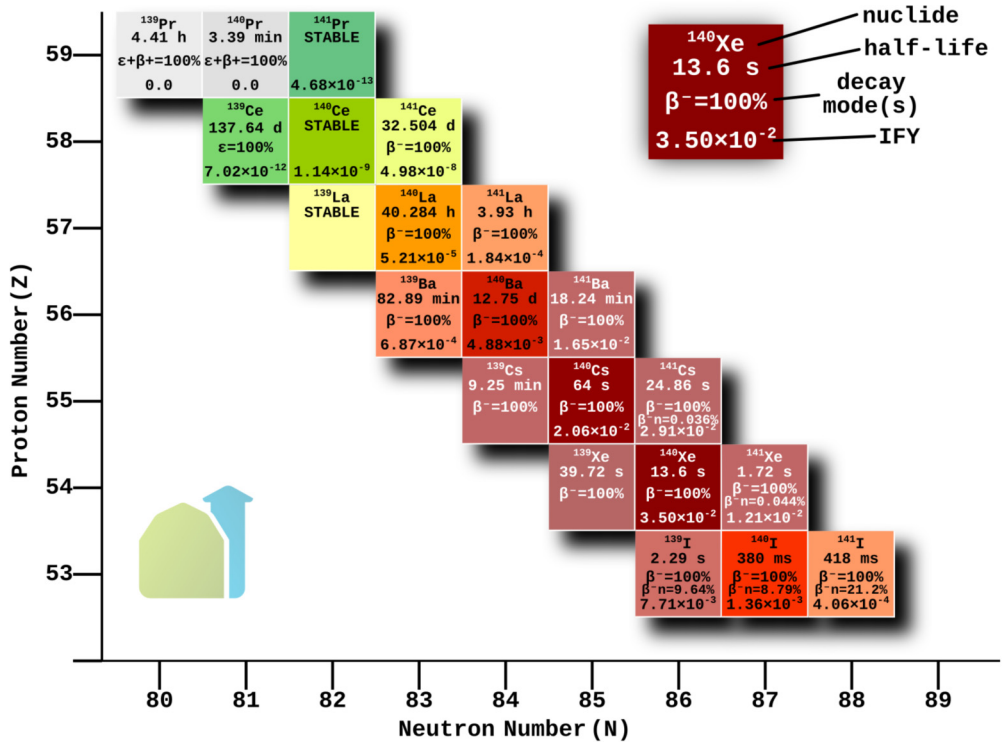

FIG. 1. Heat-map representing the independent fission yields (IFY) following thermal neutron-induced fission of ^{235}U, where mass $A = 140$ is abundantly produced. The suitable half-lives and the presence of ^{140}Xe, a noble gas that is difficult to contain, make the ^{140}Ba / ^{140}La chronometer an effective tool for estimating the zero time of a nuclear event [7].

The ENSDF evaluation [2] of ^{140}La is primarily based on the study by Chand *et al.* [11] from 1991, which used a limited two-detector setup. The DDEP evaluation uses the same data, averaging it with a number of older studies [12]. Since the work by Chand, there have been considerable advancements in the instrumentation for γ-ray spectroscopy.

This study reports results from two independent experimental campaigns. The first used the CLARION2 array at Florida State University (FSU) to identify previously unobserved low-intensity transitions and determine the intensity of known transitions. The second used the Gammasphere array at Argonne National Laboratory (ANL) to obtain precise angular information on decay levels through an angular-correlations analysis. With these complementary measurements, we aim to provide a complete characterization of the β decay of ^{140}La. We propose new recommended values for the intensities of the strongest transitions, based on this work and a number of older studies [11,13–30].

II. EXPERIMENT

Sources of ^{140}La were produced at the University of Massachusetts (UMass) Lowell research reactor through thermal-neutron irradiation of two natural La (99.9% ^{139}La) foils (total mass = 0.5 g) for 10 s. The initial activity of the produced ^{140}La was 20.5 μCi and 97 μCi for the ANL and FSU samples, respectively. Since the daughter ^{140}Ce is stable and ^{140}La was produced from nearly pure ^{139}La in a thermal neutron beam, all events observed in the spectrum can be attributed to the γ rays emitted from ^{140}La β^- decay.

A. CLARION2 measurement

The 97 μCi ^{140}La source was transferred from UMass Lowell to FSU and installed in the chamber of CLARION2 six days after irradiation. The assay of the sample was carried out over a five-day period. The CLARION2 array is a 4π array with 16 high-purity germanium (HPGe) clover detectors. Each HPGe clover detector is shielded with a bismuth germanate Compton shield. The setup and its performance are described in detail in Ref. [31].

At the time of the measurement, CLARION2 had 10 active HPGe clover detectors. Three crystals were subsequently excluded in the analysis phase because of their poorer energy resolution. The singles spectrum of the decay ^{140}La $\rightarrow$ ^{140}Ce measured with CLARION2 is given in Fig. 2. Efficiency calibrations were carried out using ^{152}Eu [32],^{133}Ba [33], and ^{24}Na [34] reference sources. We estimated a 1.5% systematic uncertainty on the intensity determination coming from the efficiency calibration, which was added in quadrature with the statistical uncertainty for the reported intensities.

Data were sorted using the CLARION2 TRINITY sorting code into a singles spectrum (1.4×10^{10} events) and a γ-γ coincidence matrix (1.7×10^{7} events). The data were analyzed using the RADWARE package GF3M, modified for matrix analysis [35]. When possible, γ-ray transitions were confirmed in coincidence spectra.

B. Gammasphere measurement

The 20.5 μCi ^{140}La source was transported from UMass Lowell to ANL, where it was installed in the Gammas-

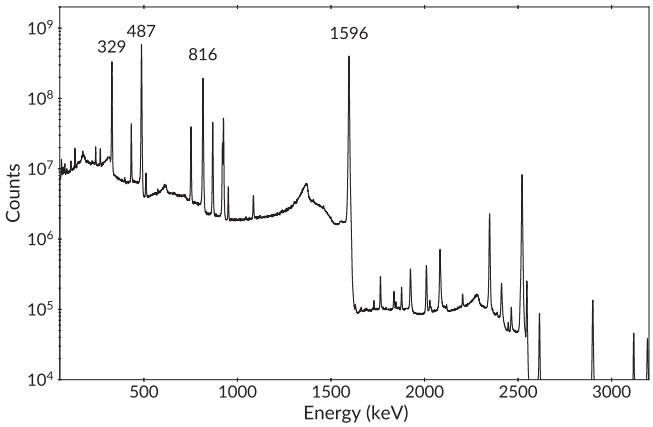

FIG. 2. Singles spectra following the decay of ^{140}La as measured with CLARION2. All visible lines correspond to the decay of ^{140}La; the strongest transitions are marked with their energy in keV.

phere array 25 hours after irradiation and assayed over a three-day period. At that time, Gammasphere had 48 active Compton-suppressed HPGe detectors. Efficiency calibrations were carried out using ^{152}Eu [32], ^{243}Am [36], ^{56}Co [37], and ^{182}Ta [38]. Well-characterized transitions were used for all four reference sources.

Data were sorted using the GSSORT package [39] into a singles spectrum (1.9×10^{10} events) and a γ-γ coincidence matrix (2.5×10^{9} events). The data were analyzed using the RADWARE package GF3M, modified for matrix analysis [35].

The 4π configuration of Gammasphere detectors allowed us to carry out angular correlation measurements for 12 different transitions. The detector pairs were split into 12 bins based on the angle θ between different Gammasphere rings. The pair combinations corresponded to $\theta = 21°$, 35°, 41°, 53°, 55°, 61°, 67°, 71°, 73°, 75°, 79°, 89°. The fitted A_2 and A_4 coefficients were extracted and matched to theoretical decay scheme values calculated from angular correlations from Yamazaki [40]. For the theoretical fit the mixing ratio, δ, was allowed to vary for the gamma ray of interest.

III. RESULTS

In this section we report results from both measurements, starting with the revised decay scheme and the intensities of the transitions. Results will be compared to the current ENSDF evaluation, largely based on the work by Chand *et al.* [11], as well as to earlier results.

Table I lists the energies, intensities and placement of the γ rays observed following the decay of ^{140}La in the current work. The intensity values were derived using two independent analysis pipelines that started from the same raw dataset. For each transition, yields were extracted in both the singles spectrum and in coincidence matrices, when possible. Within each pipeline, singles- and coincidence-based intensities were combined by a weighted average; the two pipeline results were then further averaged. The quoted uncertainty is the larger of the internal and external errors, with the calibration systematic added in quadrature. Intensities derived from the matrix were corrected for angular correlation effects. Most corrections were on the order of a percent or less, the largest being a 2% correction to the 950.9-keV transition. Intensity discussions are made with $I_\gamma(1596\ \text{keV}) = 100$. Level energies were determined through a least-squares fit to the measured γ-ray energies. We were able to determine new γ-ray transitions with an intensity as low as 0.000015 times the strongest transition. The full decay scheme is shown in Fig. 3. A total of 40 transitions were confirmed, and we propose minor adjustments to the decay scheme. In the following we will provide a justification for the proposed changes. The Appendix includes details on the angular correlations analysis (Table II) and the β-feeding values determined from γ-ray intensity balance (Table III).

A 4^+ level at 2516 keV was previously proposed [2] based on two depopulating transitions, a 432-keV γ ray populating the 4_1^+ level and a 919.5-keV γ ray populating the 2_1^+ level. In the present work, we identify an additional 166-keV transition populating the 5^+ level at 2350 keV. Support for this new transition is provided in Fig. 4, where gates on both the 242- and 267-keV transitions which depopulate the 2350-keV level reveal the 166-keV transition. The same transition and placement were proposed by Hassan *et al.* [13] based on a peak observed in coincidence with the 1596 keV transition, but not adopted in the current ENSDF evaluation [2].

A level at 2521 keV was proposed [2] on the basis of 6 depopulating transitions. We confirm the placement of the 109.6-, 173.5-, 618.8-, 925.1-, and 2521.7-keV transitions, but we find no evidence for a 438.5-keV transition. A 438.5-keV transition depopulating the 2521-keV level would populate the 2083-keV level. In a gate on the 487-keV transition which depopulates the 2083-keV level, shown in Fig. 5, there is no evidence for a 438.5-keV transition, which was previously reported with an intensity $I_\gamma(438.5\ \text{keV}) = 0.041$. For comparison, the gate clearly shows the 398-keV peak [$I_\gamma(398\ \text{keV}) = 0.071$] which also feeds the 2083-keV level. We can place a limit of $I_\gamma(438.5\ \text{keV}) < 0.005$ based on the coincidence spectrum.

A 1^+ level at 2547 keV was proposed [2] based on two depopulating transitions at 951 and 2547 keV. We confirm these, and propose a new depopulating transition at 645 keV to the 0^+ level at 1903 keV, as shown in Fig. 6. In addition, we do not confirm another transition at 1097 keV into the 1903-keV level that was previously proposed [11] from the 2^+ level at 3001 keV. For this transition, we set an upper limit on the intensity of $I_\gamma(1097\ \text{keV}) < 0.0002$ compared to the intensity of 0.024(5) previously reported in Ref. [2].

A 4^- level at 3395 keV was previously proposed [2], with one 1045-keV depopulating transition. This transition was proposed based on neutron inelastic-scattering data [41], but its placement in the level scheme was uncertain. We confirm the placement of this transition, but find a lower intensity [$I_\gamma(1045.2\ \text{keV}) = 0.014(2)$] than previously reported [0.026(15) [2]]. We also identify a new transition from this level at 982.8 keV [$I_\gamma(982.8\ \text{keV}) = 0.009(2)$], shown in Fig. 7.

Finally, we propose a new transition out of the level at 3474 keV, that was previously identified [2] based on 993-

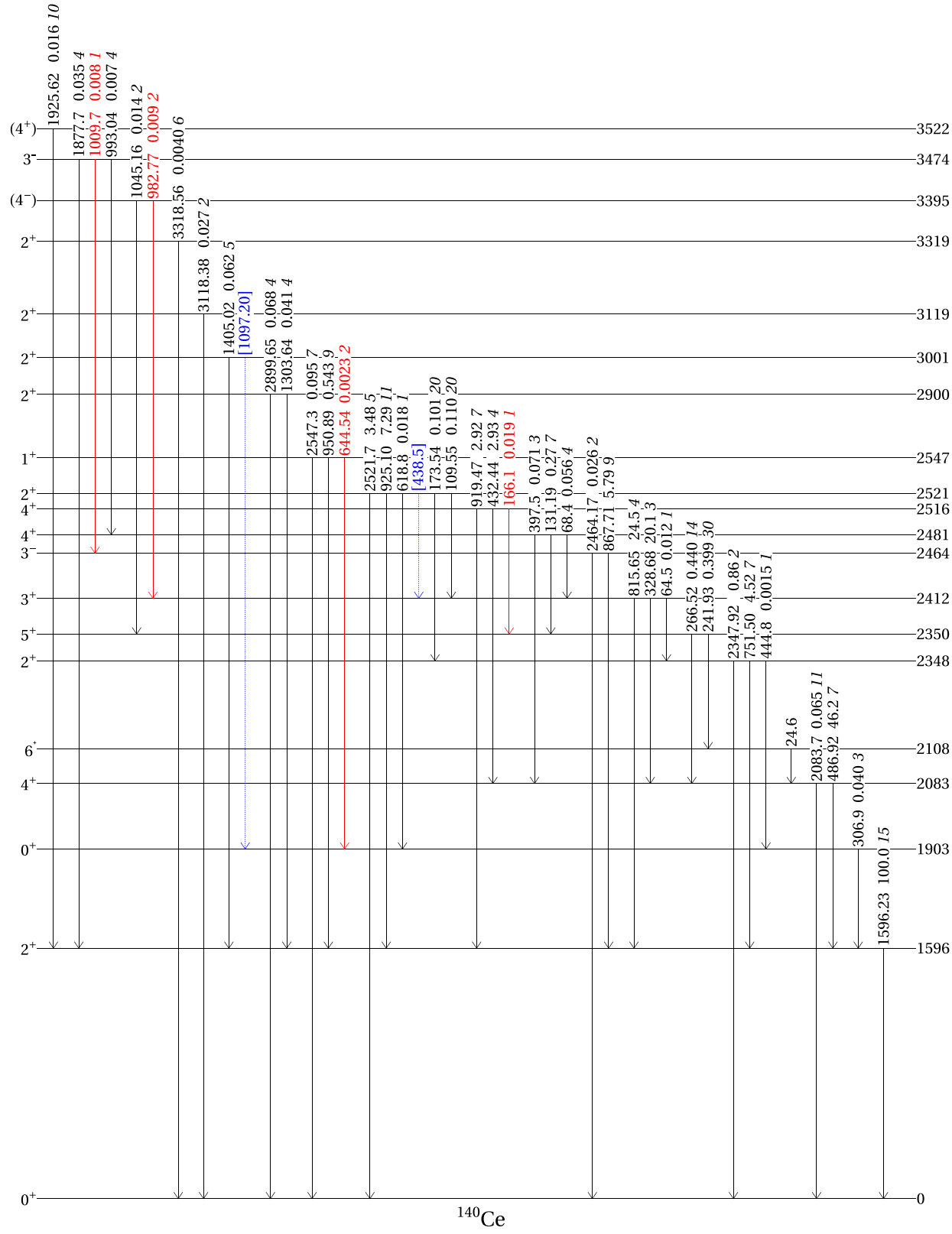

FIG. 3. Levels in ^{140}Ce populated in the β decay of ^{140}La. New transitions are highlighted in red. Transitions not observed in the present work are dashed in blue. Transitions are labeled by their energy in keV, followed by their intensity and associated uncertainties in italics.

TABLE I. Levels populated in the decay of ^{140}La into ^{140}Ce and their γ-ray transitions compared to the current ENSDF evaluation [2]. The intensities, measured with the CLARION2 array, are normalized to $I_\gamma(1596) = 100$. E_i and E_f are the initial and final levels of the γ transition, respectively. For a comparison of some of the more discrepant lines with additional literature values, see the Appendix .

J^π	E_i (keV)	E_γ (keV)	E_f (keV)	I_γ (rel)	ENSDF
2^+	1596.33(5)	1596.23(7)	0.00	100.0 (15)	100.0 (15)
0^+	1902.74(9)	306.9(5)	1596.33	0.040 (3)	0.026 (7)
4^+	2083.26(6)	486.92(7)	1596.33	46.2 (7)	47.7 (6)
		2083.7(3)	0.00	0.065 (11)	0.0121 (7)
6^+	2107.75(10)	24.6[a]	2083.26	<0.003[a]	<0.003
2^+	2347.88(5)	444.8(2)	1902.74	0.0015 (1)	0.003 (1)
		751.50(7)	1596.33	4.52 (7)	4.54 (4)
		2347.92(7)	0.00	0.86 (2)	0.89 (3)
5^+	2349.68(8)	241.93(7)	2107.75	0.399 (30)	0.434 (8)
		266.52(7)	2083.26	0.440 (14)	0.488 (8)
3^+	2411.98(6)	64.5(3)	2347.88	0.012 (1)	0.015 (2)
		328.68(7)	2083.26	20.1 (3)	21.3 (3)
		815.65(7)	1596.33	24.5 (4)	24.4 (2)
3^-	2464.11(6)	867.71(7)	1596.33	5.79 (9)	5.77 (7)
		2464.17(9)	0.00	0.026 (2)	0.012 (2)
4^+	2480.80(8)	68.4(2)	2411.98	0.056 (4)	0.079 (2)
		131.19(7)	2349.68	0.27 (7)	0.49 (1)
		397.5(1)	2083.26	0.071 (3)	0.077 (5)
4^+	2515.75(8)	166.1 (1)[b]	2349.68	0.019 (1)	
		432.44(7)	2083.26	2.93 (4)	3.04 (3)
		919.47(8)	1596.33	2.92 (7)	2.79 (3)
2^+	2521.46(5)	109.55(7)	2411.98	0.110 (20)	0.230 (4)
		173.54(7)	2347.88	0.101 (20)	0.133 (4)
		438.5[c]	2083.26	<0.005	0.041 (10)
		618.8(1)	1902.74	0.018 (1)	0.039 (4)
		925.10(4)	1596.33	7.29 (11)	7.23 (7)
		2521.7(2)	0.00	3.48 (5)	3.63 (4)
1^+	2547.24(8)	644.54(15)[b]	1902.74	0.0023 (2)	
		950.89(7)	1596.33	0.543 (9)	0.544 (7)
		2547.3(2)	0.00	0.095 (7)	0.106 (3)
2^+	2899.77(6)	1303.64(11)	1596.33	0.041 (4)	0.044 (7)
		2899.65(7)	0.00	0.068 (4)	0.070 (2)
2^+	3001.35(9)	1097.20[c]	1902.74	<0.0002	0.024 (5)
		1405.02(7)	1596.33	0.062 (5)	0.062 (7)
2^+	3118.60(8)	3118.56(8)	0.00	0.027 (2)	0.026 (1)
2^+	3318.60(8)	3318.38(8)	0.00	0.0040 (6)	0.0040 (3)
(4^-)	3394.83(10)	982.77(15)[b]	2411.98	0.009 (2)	
		1045.16(7)	2349.68	0.014 (2)	0.026 (15)
3^-	3473.85(9)	993.04(8)	2480.80	0.007 (4)	0.014 (5)
		1009.7(1)[b]	2464.11	0.008 (1)	
		1877.7(2)	1596.33	0.035 (4)	0.043 (4)
(4^+)	3521.96(10)	1925.62(9)	1596.33	0.016 (10)	0.014 (2)

[a]From level energy difference. Transition not observed but implied by coincidence analysis. The limit on the intensity, used for the β feedings in Table III of the Appendix, was adopted from Ref. [15].
[b]Newly observed γray.
[c]Transition not observed in this work. Energy from level-energy difference.

and 1878-keV depopulating transitions. This transition at 1010 keV, shown in Fig. 8, populates the level at 2464 keV.

A separate discussion needs to be made about the 2083.7-keV $E4$ transition, for which we measured an intensity that is 2 to 9 times larger than the majority of other measurements. Accurately determining the intensity of this transition is particularly challenging because of the presence of two strong transitions, at 486.9 ($I_\gamma = 46$) and 1596.2 keV ($I_\gamma = 100$), whose energies sum to the energy of the peak in question. We estimated the contribution of random and true coincidences by comparing it with the summing peaks of other strong transitions (1596–1596, 1596–816) which do not have a corresponding peak at the sum energy. The intensity reported in Table I was obtained by subtracting the coincidence summing contributions rescaled with the detection efficiency.

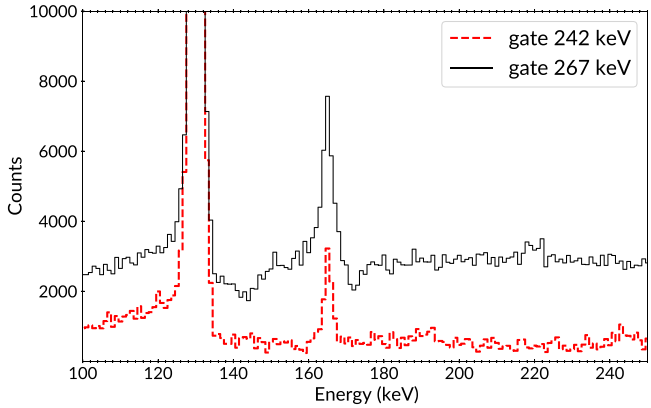

FIG. 4. A new transition at 166 keV is proposed that depopulates the level at 2516 keV, which was confirmed by gating on the two transitions out of the 2350-keV level. The strong 131-keV transition populating the 2350-keV level is also visible in the gated spectra.

Angular correlation results for a few chosen transitions are presented in Fig. 9 and numerical results are given in Table II of the Appendix. As shown in Fig. 9(a), the well established 4-2-0 cascade of 487–1596 keV shows excellent agreement with the theoretical prediction. Similarly, for the 752–1596 keV cascade of spins 2-2-0, the angular correlation analysis gives a mixing ratio of $\delta = 0.35(1)$ for the 752-keV transition, which is in excellent agreement with the values of 0.38(4) from β decay and 0.31^{+34}_{-14} from $(n, n'\gamma)$ [2].

For the 432–487 keV, 4-4-2 cascade, there is a single measurement [2] of the 432-keV mixing ratio of $\delta = -0.04(2)$, indicating nearly pure $M1$ character. The present angular correlation analysis confirms the prior result, yielding a mixing ratio of 0.01(3). The 329-keV transition is part of a 3-4-2 cascade, and its mixing ratio was previously determined as $-0.049(6)$ in β decay and either 0.19(4) or 13^{+11}_{-5} in $(n, n'\gamma)$ [41]. The present analysis favors the solution of nearly pure $M1$ character with $\delta = -0.07(2)$.

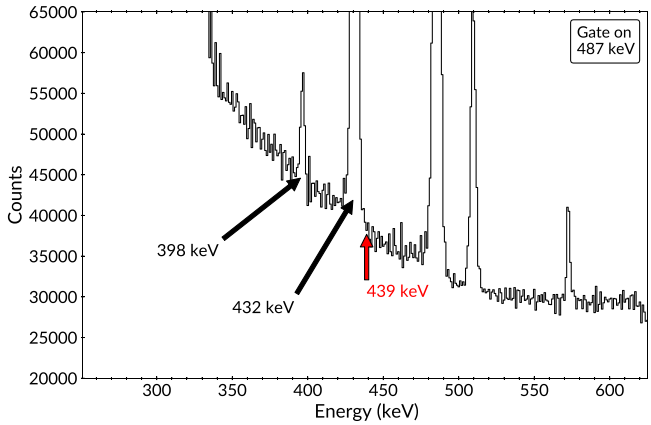

FIG. 5. Spectrum obtained with a gate on the 487-keV transition, showing a 398-keV transition, but no evidence for a 438.5-keV gamma, previously reported with a similar intensity.

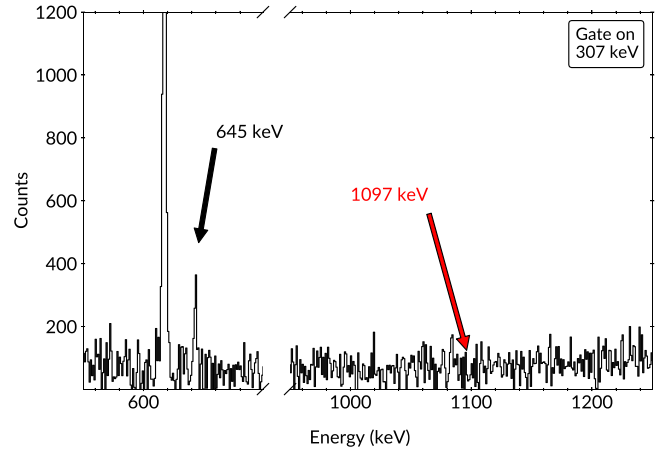

FIG. 6. Spectrum obtained with a gate on the 307-keV peak out of the 1903-keV level. A proposed new transition is visible at 645 keV, but we see no signs of a peak around 1097 keV.

IV. DISCUSSION

The importance of ^{140}La in societal applications is evident from the more than 20 experiments conducted over the past 70 years to characterize its decay. As mentioned previously, the DDEP evaluation attempts to incorporate some of the data from literature, while the latest ENSDF evaluation adopts data from the most recent work by Chand *et al.* [11].

In an effort to consider the full body of data available on ^{140}La decay, we performed a comprehensive literature search of measured γ-ray intensities. Our focus is on the three most intense transitions, which are the most likely to be used to identify and quantify ^{140}La in nuclear forensics and other applications. Numerical values, along with the recommended relative intensities, are summarized in Table V of the Appendix.

The strongest transition at 1596 keV is often reported with an intensity of 100, to which all other intensities are normalized. To convert these to absolute values, one can obtain a normalization factor by summing the total flux of transitions populating the ground state, of which the 1596-keV

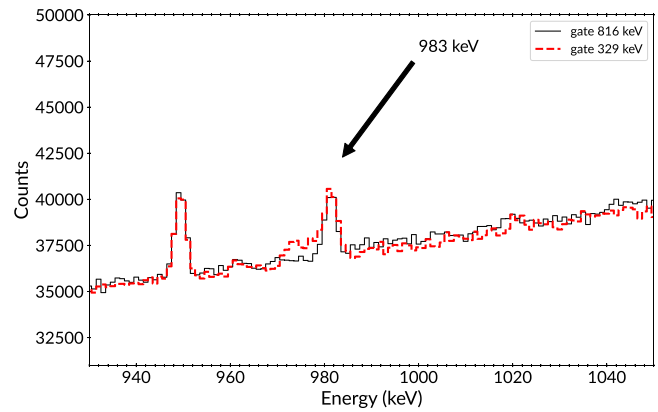

FIG. 7. A new 983-keV transition is proposed depopulating the level at 3395 keV, confirmed by gating on the 816- and 329-keV transitions out of the 2412-keV level.

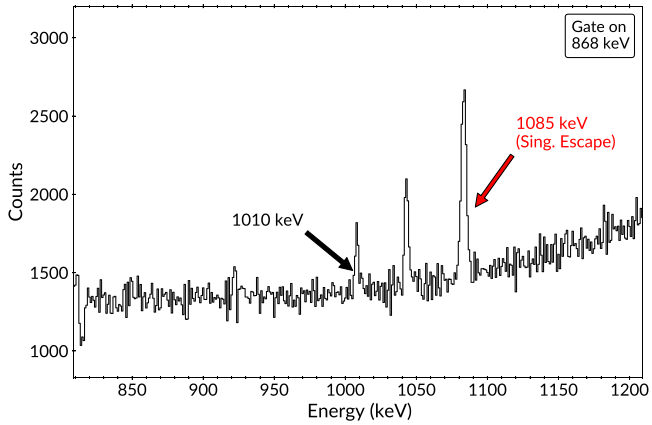

FIG. 8. A new 1010-keV transition is proposed depopulating the level at 3474 keV, confirmed by gating on the 868-keV transition out of the 2464-keV level. The single-escape peak from the strong 1596-keV transition can also be seen in the gate.

transition is the main contributor. This method, which was used to provide absolute intensities in most of the literature data [14,19,23,24], is possible because the direct beta decay to the ground state is negligible, as it is a highly forbidden decay ($3^- \rightarrow 0^+$). Using this approach, we determine that the 1596-keV transition is observed in 95.49(8)% of ^{140}La decays, in excellent agreement with the value of 95.40(8)% adopted in the current evaluation from Debertin *et al.* [2,19]. While the sub-0.1% uncertainty applies to this transition, it reflects cancellation effects between the two highly correlated quantities I_γ(1596 keV) and the normalization, as discussed in detail in Ref. [42]. We obtain a normalization factor of 0.955(14) to convert to absolute values the intensities of all γ rays that *do not* directly populate the ground state. Debertin *et al.* only estimated the contribution to the conversion factor of some weak transitions to the ground state that we were able to measure directly. For this reason we recommend our absolute I_γ(1596 keV) and the normalization factor. Absolute

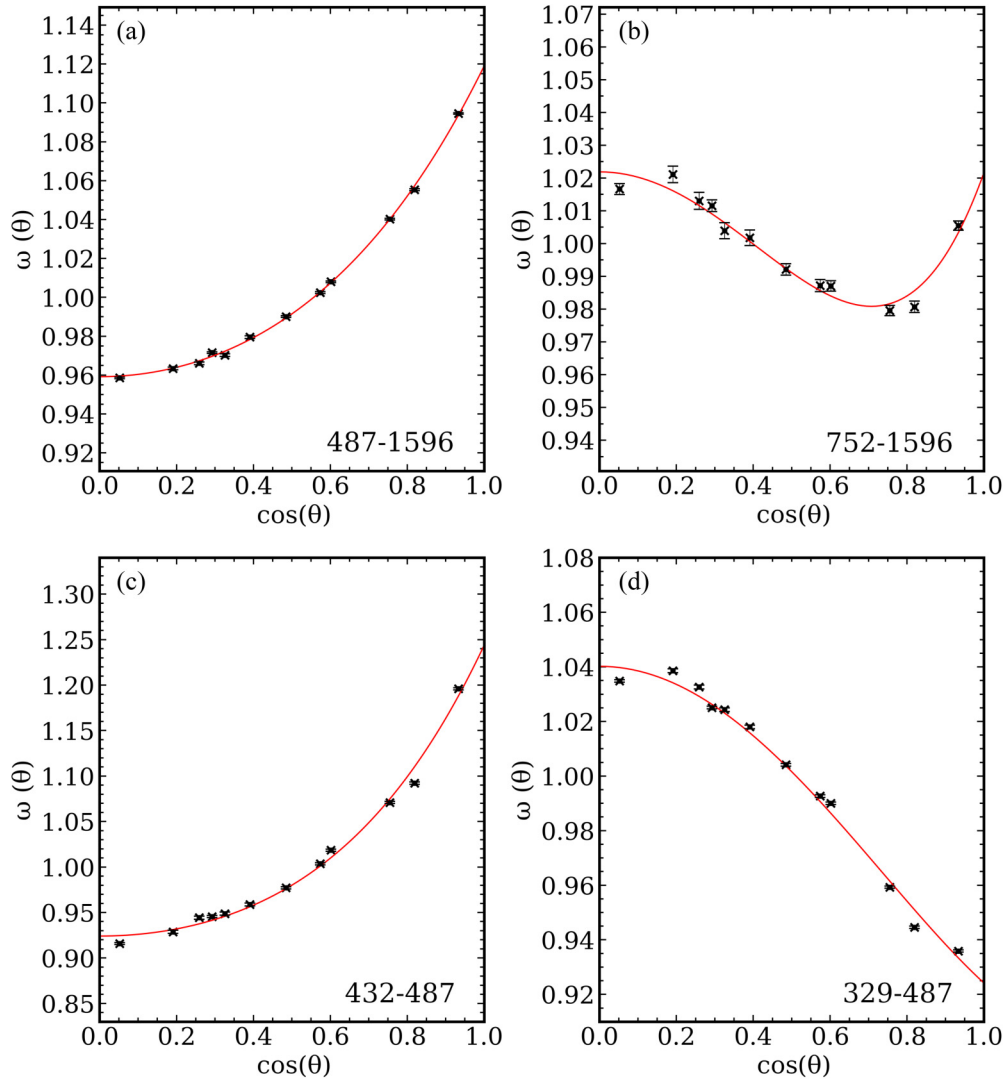

FIG. 9. Angular correlation plots measured with Gammasphere for the cascades (a) 487-1596 (b) 752-1596 (c) 432-487 (d) 329-487. The red solid line represents a fit to the data points. Respective δ and A_2 and A_4 values are listed in the Appendix.

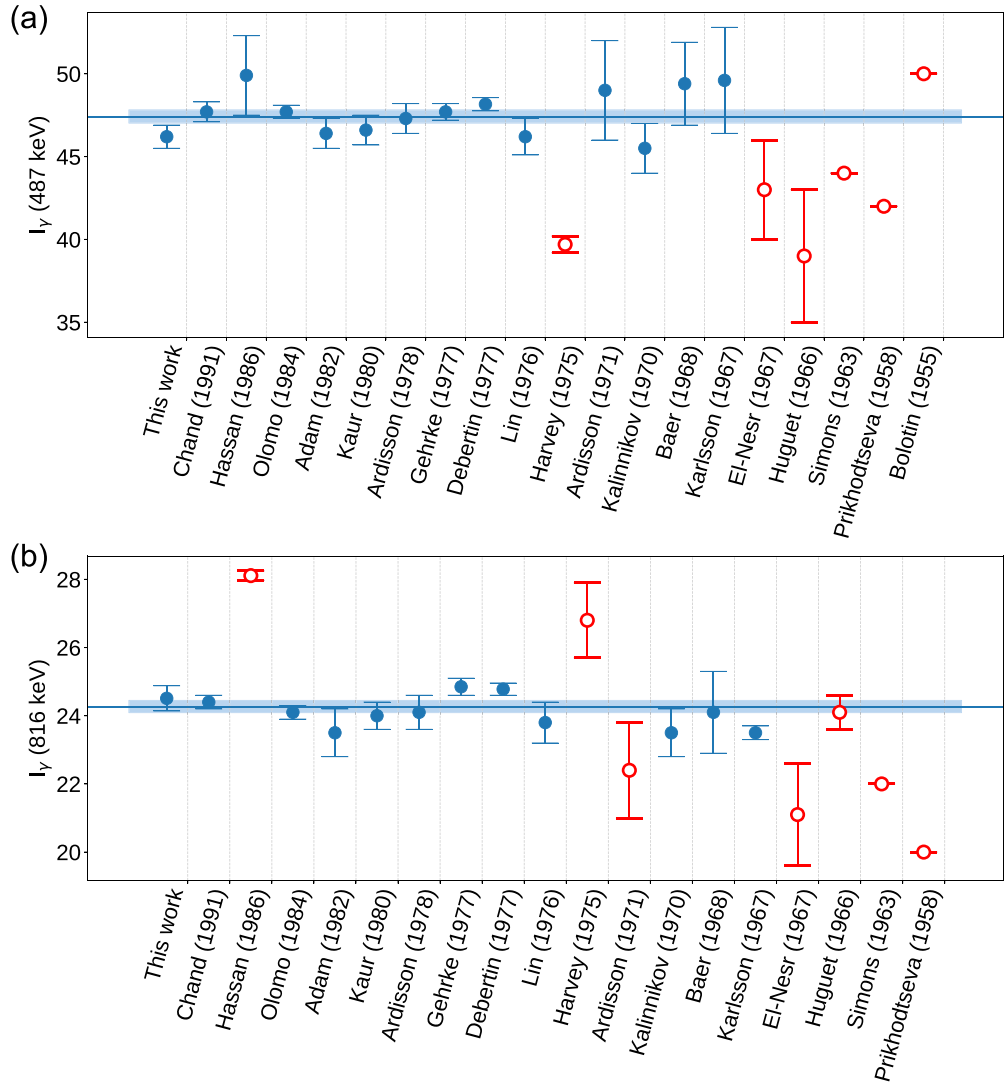

FIG. 10. Relative intensities of the 487- (a) and 816-keV (b) transitions from the decay of ^{140}La reported in the literature. Intensities are normalized to $I_\gamma(1596) = 100$. The horizontal line is the weighted average of the experimental measurements. Older and discrepant data points, in red, have been excluded from the average based on a statistical analysis. For absolute intensities, we recommend a conversion factor of 0.955(14), based on our estimated total flux of transitions to the ground state. The literature data are labeled on the abscissa by author and year; these labels correspond to the following references: Chand (1991) [11]; Hassan (1986) [13]; Olomo (1984) [14]; Adam (1982) [15]; Kaur (1980) [16]; Ardisson (1978) [17]; Gehrke (1977) [18]; Debertin (1977). [19]; Lin (1976) [20]; Harvey (1975) [21]; Ardisson (1971) [22]; Kalinnikov (1970) [23]; Baer (1968) [24]; Karlsson (1967) [25]; El-Nesr (1967) [26]; Huguet (1966) [27]; Simons (1963) [28]; Prikhodtseva (1958) [29]; and Bolotin (1955) [30].

intensities for all transitions are reported in Table V of the Appendix.

The next strongest transition is the one at 487 keV. As shown in Fig. 10(a), there are large fluctuations in the measured data. The weighted average for the relative intensity is $I_\gamma(487\ \text{keV}) = 47.42(40)$, which we calculated after excluding outliers based on their large contribution to the total χ^2 [21,26,27] and older measurements reported without uncertainties [28–30], shown in red in Fig. 10(a). Our recommended absolute intensity is 45.3 (8)%, which agrees well with the value of 45.5(6)% currently recommended in ENSDF.

The third-strongest transition is at 816 keV, and measured data are shown in Fig. 10(b), where we notice once again the spread among previous results, even those reported with high precision. Also in this case, discrepant data points [13,21,22,26] and older data [27–29], in red in Fig. 10(b), have been excluded from the weighted average. One additional data point reported in Ref. [30] with $I_\gamma = 46$ has not been plotted, for clarity. The recommended relative intensity for this transition is $I_\gamma(816\ \text{keV}) = 24.27(18)$. Our recommended absolute intensity is 23.2(4)%, in good agreement with the ENSDF value of 23.3(2)%.

Using the same method, we also provide a recommended value for the transition at 329 keV. The recommended absolute intensity is $I_\gamma(329\ \text{keV}) = 20.1(4)\%$, based on the weighted average of the relative intensities $I_\gamma(329\ \text{keV}) = 21.0(2)$. In this case, the spread of the data points is even

broader, and we excluded from the weighted average values from Refs. [25,27]. A figure showing all data points and the resulting average is presented in Fig. 11 of the Appendix.

V. CONCLUSION

In this work, we performed high-precision gamma-ray spectroscopy of ^{140}La using the Gammasphere and CLARION2 arrays. Our analysis identified a total of 40 transitions, including three previously unreported transitions.

We updated the decay scheme of ^{140}La and provided recommended γ-ray intensities for the strongest transitions based on both our experimental data and a comprehensive reevaluation of past measurements. The revised intensity values of the most prominent transitions at 328.7, 486.9, and 815.7 keV are in general agreement with recent evaluations. While the central values remain close to those compilations, our recommendations supply a single set that resolves minor inconsistencies across sources and is accompanied by an explicitly propagated uncertainty.

The high-statistics measurement conducted with Gammasphere also allowed us to perform an angular correlation analysis, which generally confirmed the level assignments and spin-parity designations in the decay of ^{140}La.

ACKNOWLEDGMENTS

This work was supported by the U.S. Department of Energy, National Nuclear Security Administration, Office of Defense Nuclear Nonproliferation Research and Development (DNN R&D), and by the Office of Nuclear Physics, Office of Science of the U.S. Department of Energy, under Contracts No. DE-SC0012704 (Brookhaven National Laboratory), No. DE-AC02-06CH11357 (Argonne National Laboratory) and No. DE-AC05-00OR22725 (Oak Ridge National Laboratory). This research used resources of the Argonne National Laboratory's ATLAS facility, which is a U.S. Department of Energy, Office of Science User Facility. This project was supported in part by the U.S. Department of Energy, Office of Science, Office of Workforce Development for Teachers and Scientists (WDTS) under the Science Undergraduate Laboratory Internships Program (SULI). The research described herein is Fundamental Research as defined in the ITAR [22 CFR 120.34(a)(8)], EAR (15 CFR 734.8), or Part 810 (10 CFR 810.3), as applicable, and as described in the USD (AT&L) memoranda on Fundamental Research, dated May 24, 2010, and on Contracted Fundamental Research, dated June 26, 2008.

DATA AVAILABILITY

The data that support the findings of this article are not publicly available upon publication because it is not technically feasible and/or the cost of preparing, depositing, and hosting the data would be prohibitive within the terms of this research project. The data are available from the authors upon reasonable request.

APPENDIX

See Tables II–V for additional information on angular correlation analysis, β-feeding, a literature review of the available intensities for the strongest transitions following ^{140}La β-decay and the absolute intensities for 100 decays obtained from our work. See Fig. 11 for the relative intensities of the 329-keV transition from the decay of ^{140}La reported in the literature.

TABLE II. Summary of angular correlation analysis. γ_g is the gating transition and γ_a is the analyzed transition. The third column gives the spins used in the analysis, while the fourth, fifth, and sixth columns respectively give the mixing ratio of the γ_a transition and the A_2, A_4 coefficients resulting from the Legendre fit to the data. The last column gives the evaluated values of mixing ratios if available. We selected (γ_g, γ_a) pairs that yielded well-resolved coincidence peaks with sufficient statistics for a reliable fit.

γ_g (keV)	γ_a (keV)	J_i-J-J_f	δ	A_2	A_4	δ^{lit} [2]
1596	487	0-2-4		0.102(3)	0.0092(5)	
	752	0-2-2	0.35(1)	−0.0145(9)	0.036(2)	0.38(4)
	816	0-2-3	−0.02(1)	−0.091(1)	0.0012(9)	−0.03(1)
	868	0-2-3	0.01(1)	−0.067(1)	0.004(1)	
	919	0-2-4		0.12(1)	0.015(4)	
	925	0-2-2	−0.18(1)	0.354(8)	0.011(1)	−0.22(4)
	951	0-2-1	0.003(4)	−0.26(1)	0.021(5)	0.01(7)
487	432	4-2-4	0.01(3)	0.198(8)	0.03(1)	−0.04(2)
	329	4-2-3	−0.07(2)	−0.083(4)	0.012(1)	−0.049(6)
	267	4-2-5	0.06(3)	−0.028(2)	0.031(2)	−0.14(12)
131	267	4-5-4	−0.02(3)	0.079(3)	0.035(4)	−0.13(5)
110	329	2-3-4	0.33(5)	−0.049(5)	0.011(7)	0.26(2)

TABLE III. Energy levels and corresponding β-feeding values determined from γ-ray and conversion-electron intensity balance; our results are compared with literature values from [2].

Energy level (keV)	I_{β^-} (%)	$I_{\beta^-}^{\mathrm{lit}}$ [2] (%)
1596.33	7.1(17)	5.9(16)
1902.74	0.019(4)	<0.002
2083.26	20.3(14)	20.2(9)
2347.88	4.98(12)	4.97(5)
2349.68	0.44(15)	0.207(25)
2411.98	43.2(8)	43.9(4)
2464.11	5.55(12)	5.52(7)
2480.80	0.70(12)	1.124(20)
2515.75	5.67(12)	5.63(5)
2521.46	10.66(20)	11.05(8)
2547.24	0.613(23)	0.622(8)
2899.77	0.104(6)	0.109(7)
3001.35	0.059(5)	0.082(9)
3118.60	0.0258(20)	0.0248(10)
3318.60	0.0038(6)	0.0038(3)
3394.83	0.022(3)	0.025(15)
3473.85	0.048(6)	0.054(7)
3521.96	0.015(10)	0.0134(19)

TABLE IV. Comparison of the intensities of the most intense transitions following ^{140}La β decay as reported in the literature. Intensities are normalized to $I_\gamma(1596) = 100$. Earlier data, as well as discrepant data (in italics) have not been included in the weighted average. For absolute intensities, we recommend a conversion factor of 0.955(14), based on our estimated total flux of transitions to the ground state.

Energy (keV)	This work	Evaluated intensity	1991CH05 [11]	1986HA20 [13]	1984OL08 [14]	1982AD02 [15]	1980KA32 [16]	1978AR28 [17]	1977GE12 [18]	1977DE34 [19]	1976LI06 [20]	1975HA50 [21]	1971AR35 [22]	1970KA18 [23]	1968BA18 [24]	1967KA12 [25]	1967EL01 [26]	1966HU18 [27]	1963SI11 [28]	1958PR68 [29]	1955BO85 [30]
328.7	20.1(3)	21.04(21)	21.1(3)	22.6(11)	21.5(2)	21.7(4)	21.50(36)	21.5(6)	21.46(22)	21.74(19)	21.2(6)	18.8(5)	19.9(13)	19.4(6)	21.4(11)	*25.4(20)*	20.0(2)	*31(3)*	*19*		*40*
486.9	46.2(5)	47.42(40)	47.7(6)	49.9(24)	47.7(4)	46.4(9)	46.55(88)	47.3(9)	47.7(5)	48.16(40)	46.2(11)	*39.7(5)*	49(3)	45.0(15)	49.4(25)	49.6(32)	*43(3)*	*39(4)*	*44*	*42*	*50*
815.7	24.5(3)	24.27(18)	24.4(2)	*28.11(14)*	24.1(2)	23.5(7)	24.0(4)	24.1(5)	24.85(25)	24.78(18)	23.8(6)	*26.8(11)*	*22.4(14)*	23.5(7)	24.1(12)	23.5(2)	*21.1(15)*	*24.1(5)*	*22*	*20*	*46*

TABLE V. Levels populated in the decay of ^{140}La to ^{140}Ce and the corresponding γ-ray transitions, with absolute intensities per 100 decays determined from our work. E_i and E_f are the populated and final levels of the γ transition, respectively. Recommended values are based on a combined analysis of all available literature data and the present results.

J^π	E_i (keV)	E_γ (keV)	E_f (keV)	I_γ (%)	Recommended
2^+	1596.33(5)	1596.23(7)	0.00	95.49 (8)	95.49 (8)
0^+	1902.74(9)	306.9(5)	1596.33	0.038 (3)	
4^+	2083.26(6)	486.92(7)	1596.33	44.1 (9)	45.3 (8)
		2083.7(3)	0.00	0.062 (11)	
6^+	2107.75(10)	24.6[a]	2083.26	<0.0029[a]	
2^+	2347.88(5)	444.8(2)	1902.74	0.00143 (10)	
		751.50(7)	1596.33	4.32 (9)	
		2347.92(7)	0.00	0.821 (22)	
5^+	2349.68(8)	241.93(7)	2107.75	0.38 (3)	
		266.52(7)	2083.26	0.419 (15)	
3^+	2411.98(6)	64.5(3)	2347.88	0.0115 (10)	
		328.68(7)	2083.26	19.2 (4)	20.1 (4)
		815.65(7)	1596.33	23.4 (5)	23.2 (4)
3^-	2464.11(6)	867.71(7)	1596.33	5.53 (12)	
		2464.17(9)	0.00	0.0248 (20)	
4^+	2480.80(8)	68.4(2)	2411.98	0.053 (4)	
		131.19(7)	2349.68	0.26 (7)	
		397.5(1)	2083.26	0.068 (3)	
4^+	2515.75(8)	166.1 (1)[b]	2349.68	0.0181 (10)	
		432.44(7)	2083.26	2.80 (6)	
		919.47(8)	1596.33	2.79 (8)	
2^+	2521.46(5)	109.55(7)	2411.98	0.105 (19)	
		173.54(7)	2347.88	0.0965 (24)	
		438.5[c]	2083.26	<0.0048	
		618.8(1)	1902.74	0.0172 (10)	
		925.10(4)	1596.33	6.96 (15)	
		2521.7(2)	0.00	3.32 (7)	
1^+	2547.24(8)	644.54(15)[b]	1902.74	0.00220(20)	
		950.89(7)	1596.33	0.519 (21)	
		2547.3(2)	0.00	0.091 (7)	
2^+	2899.77(6)	1303.64(11)	1596.33	0.039 (4)	
		2899.65(7)	0.00	0.065 (4)	
2^+	3001.35(9)	1097.20[c]	1902.74	<0.00019	
		1405.02(7)	1596.33	0.059 (5)	
2^+	3118.60(8)	3118.56(8)	0.00	0.0258 (20)	
2^+	3318.60(8)	3318.38(8)	0.00	0.0038 (6)	
(4^-)	3394.83(10)	982.77(15)[b]	2411.98	0.0086 (19)	
		1045.16(7)	2349.68	0.0134 (19)	
3^-	3473.85(9)	993.04(8)	2480.80	0.007 (4)	
		1009.7(1)[b]	2464.11	0.0076 (10)	
		1877.7(2)	1596.33	0.033 (4)	
(4^+)	3521.96(10)	1925.62(9)	1596.33	0.015 (10)	

[a]From level energy difference. Transition not observed but implied by coincidence analysis. The limit on the intensity, used for the β feedings in Table III, was adopted from Ref. [15].

[b]Newly observed γ ray.

[c]Transition not observed in this work. Energy from level-energy difference.

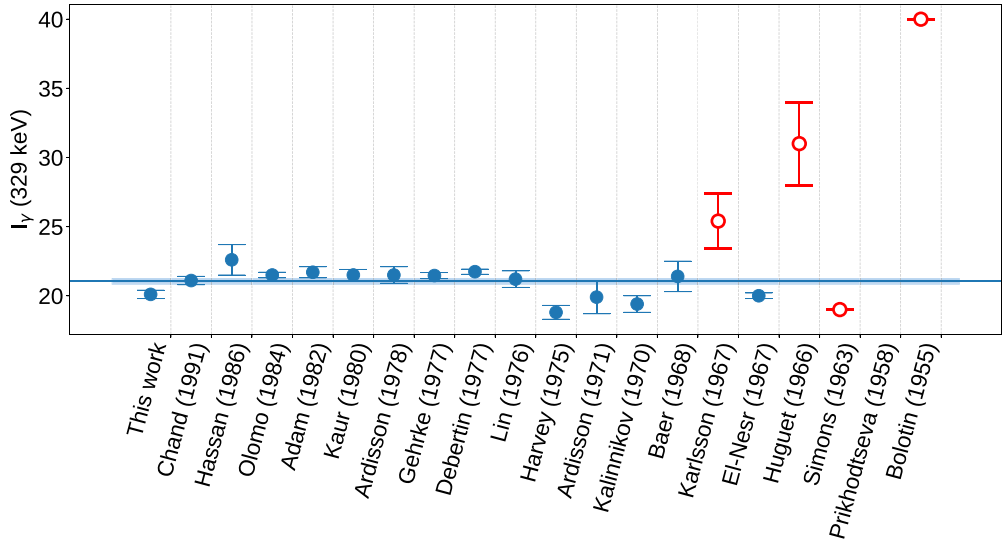

FIG. 11. Relative intensities of the 329-keV transition from the decay of ^{140}La reported in the literature. Intensities are normalized to $I_\gamma(1596) = 100$. The horizontal line is the weighted average of the experimental measurements. Older and discrepant data points, in red, have been excluded from the average based on a statistical analysis. For absolute intensities, we recommend a conversion factor of 0.955(14). The literature data are labeled on the abscissa by author and year; these labels correspond to the following references: Chand (1991) [11]; Hassan (1986) [13]; Olomo (1984) [14]; Adam (1982) [15]; Kaur (1980) [16]; Ardisson (1978) [17]; Gehrke (1977) [18]; Debertin (1977) [19]; Lin (1976) [20]; Harvey (1975) [21]; Ardisson (1971) [22]; Kalinnikov (1970) [23]; Baer (1968) [24]; Karlsson (1967) [25]; El-Nesr (1967) [26]; Huguet (1966) [27]; Simons (1963) [28]; Prikhodtseva (1958) [29]; and Bolotin (1955) [30].

[1] G. P. A. Nobre, R. Capote, M. T. Pigni, *et al.*, ENDF/B-VIII.1: Updated nuclear reaction data library for science and applications arXiv:2511.03564.

[2] N. Nica, Nuclear data sheets for A = 140, Nucl. Data Sheets **154**, 1 (2018).

[3] P. Jansson, S. J. Svärd, A. Håkansson, and A. Bäcklin, A device for nondestructive experimental determination of the power distribution in a nuclear fuel assembly, Nucl. Sci. Eng. **152**, 76 (2006).

[4] F. Padoani, P. Karhu, F. Medici, B. Wernsperger, and R. Werzi, Setting up and implementation of a global atmospheric radioactivity monitoring network for CTBT verification purposes, J. Radiol. Nucl. Chem. **263**, 183 (2005).

[5] K. Yamba, O. Sanogo, M. B. Kalinowski, M. Nikkinen, and J. Koulidiati, Fast and accurate dating of nuclear events using La-140/Ba-140 isotopic activity ratio, Appl. Radiat. Isot. **112**, 141 (2016).

[6] J.-H. Moon, S.-P. Hong, and K. B. Dasari, Investigation of uranium analysis using ^{140}Ba/^{140}La induced from ^{235}U fission reaction, J. Radiol. Nucl. Chem. **333**, 6605 (2024).

[7] S. Pommé, S. Collings, A. Harms, *et al.*, Fundamental uncertainty equations for nuclear dating applied to the ^{140}Ba - ^{140}La and ^{227}Th - ^{223}Ra chronometers, J. Environ. Radioact. **162-163**, 358 (2016).

[8] J. K. Tuli, Evaluated nuclear structure data file, Nucl. Instrum. Methods Phys. Res. Sect. A **369**, 506 (1996).

[9] R. Helmer, International decay data evaluation project, Nucl. Instrum. Methods Phys. Res. Sect. A **422**, 518 (1999).

[10] W. Huang, M. Wang, F. G. Kondev, G. Audi, and S. Naimi, The AME 2020 atomic mass evaluation (I). Evaluation of input data, and adjustment procedures, Chin. Phys. C **45**, 030002 (2021).

[11] B. Chand, J. Goswamy, D. Mehta, N. Singh, and P. Trehan, Study of the radioactive decays of ^{140}Ba and ^{140}La, Can. J. Phys. **69**, 90 (1991).

[12] V. P. Chechev and N. K. Kuzmenko, Decay data evaluation project (DDEP): Updated evaluation of the ^{133}Ba, ^{140}Ba, ^{140}La and ^{141}Ce decay characteristics, EPJ Web Conf. **146**, 02048 (2017).

[13] A. Hassan, S. Abdel-Malak, M. Abou-Leila, A. Sroor, and H. Ismail, The level structure of ^{140}Ce, Acta Phys. Hung. **60**, 3 (1986).

[14] J. B. Olomo and T. D. MacMahon, Gamma-ray emission probabilities in the decay of ^{140}Ba and ^{140}La, J. Phys. (London) **E17**, 124 (1984).

[15] I. Adam, N. M. Antoneva, V. B. Brudanin, M. Budzynski, T. Vylov, V. A. Dzhashi, A. Zhumamuratov, A. I. Ivanov, V. G. Kalinnikov, A. Kugler, V. V. Kuznetsov, L. Z. Sik, T. M. Muminov, A. F. Novgorodov, Y. N. Podkopaev, Z. D. Shavgulidze, and V. L. Chikhladze, Study of the radioactive decay of isobars with mass A = 140, Bulletin of the Academy of Sciences of the USSR **46**, 136 (1982).

[16] R. Kaur, A. K. Sharma, S. S. Sooch, and P. N. Trehan, Level structure of ^{140}Ce from the decay of ^{140}La, J. Phys. Soc. Jpn. **49**, 2122 (1980).

[17] G. Ardisson, Intensites des γ associes a la decroissance de ^{140}La, Nucl. Instrum. Methods **151**, 505 (1978).

[18] R. J. Gehrke, R. G. Helmer, and R. C. Greenwood, Precise relative γ-ray intensities for calibration of Ge semiconductor detectors, Nucl. Instrum. Methods **147**, 405 (1977).

[19] K. Debertin, U. Schotzig, and K. F. Walz, Gamma-ray emission probabilities in the decay of barium-140 and lanthanum-140, Nucl. Sci. Eng. **64**, 784 (1977).
[20] C.-C. Lin, γ-Ray intensities in the decay of ^{140}Ba - ^{140}La and ^{152}Eu: Use of 13 y ^{152}Eu as a secondary calibration standard, J. Inorg. Nucl. Chem. **38**, 1409 (1976).
[21] J. T. Harvey, J. L. Meason, J. C. Hogan, and H. L. Wright, Gamma-ray intensities for the radioactive decay of barium-140 and lanthanum-140, Nucl. Sci. Eng. **58**, 431 (1975).
[22] G. Ardisson and C. Marsol, Experimental study of nuclear levels of ^{140}Ce formed in decay of ^{140}La, Rev. Roum. Phys. **16**, 1045 (1971).
[23] V. Kalinnikov, H. Ravn, H. Hansen, and N. Lebedev, Levels of ^{140}Ce excited during the decay of ^{140}La and ^{140}Pr, Bulletin of the Academy of Sciences of the USSR **34**, 815 (1970).
[24] H. W. Baer, J. Reidy, and M. L. Wiedenbeck, The decay of ^{140}La to levels in ^{140}Ce, Nucl. Phys. A **113**, 33 (1968).
[25] S.-E. Karlsson, B. Svahn, H. Pettersson, G. Malmsten, and E. Y. D. Aisenberg, The decay of ^{140}La, Nucl. Phys. A **100**, 113 (1967).
[26] M. El-Nesr and M. El-Aassar, Further study on γ transitions in ^{140}Ce, Z. Naturforsch. **22**, 299 (1967).
[27] M. Huguet, H. Forest, and C. Ythier, Sur l'etude du rayonnement γ de haute energie au moyen d'un spectrometre a paires a haute resolution, Compt. Rend. **263**, 79 (1966).
[28] L. Simons, K. E. Nysten, P. Holmberg, H. Jungner, A. Anttila, S. Bergstrom, and E. Hagebo, Gamma-gamma directional correlations of ^{140}Ce, Acta Polytech. Scand. Phys. Nucl. Ser. Vol No. 22 Univ. of Helsinki, 1962.
[29] V. P. Prikhodtseva and I. V. Kholnov, Gamma-spectrum of ^{140}La, Bulletin of the Academy of Sciences of the USSR **22**, 176 (1958).
[30] H. H. Bolotin, C. H. Pruett, P. L. Roggenkamp, and R. G. Wilkinson, Excited states of ^{140}Ce, Phys. Rev. **99**, 62 (1955).
[31] T. J. Gray, J. M. Allmond, D. T. Dowling, M. Febbraro, T. T. King, S. D. Pain, D. W. Stracener, S. Ajayi, J. Aragon, L. Baby, *et al.*, CLARION2-TRINITY: A Compton-suppressed hpge and GAGG: Ce-Si-Si array for absolute cross-section measurements with heavy ions, Nucl. Instrum. Methods Phys. Res. Sect. A **1041**, 167392 (2022).
[32] M. J. Martin, Adopted levels, gammas for ^{152}Sm, Nucl. Data Sheets **114**, 1497 (2013).
[33] Y. Khazov, A. Rodionov, and F. Kondev, Nuclear data sheets for A = 133, Nucl. Data Sheets **112**, 855 (2011).
[34] M. S. Basunia and A. Chakraborty, Nuclear data sheets for A=24, Nucl. Data Sheets **186**, 3 (2022).
[35] D. Radford, ESCL8R and LEVIT8R: Software for interactive graphical analysis of hpge coincidence data sets, Nucl. Instrum. Methods Phys. Res. Sect. A **361**, 297 (1995).
[36] M. Basunia, Nuclear data sheets for A = 237, Nucl. Data Sheets **107**, 2323 (2006).
[37] H. Junde, H. Su, and Y. Dong, Nuclear data sheets for A = 56, Nucl. Data Sheets **112**, 1513 (2011).
[38] B. Singh, Nuclear data sheets for A = 182, Nucl. Data Sheets **130**, 21 (2015).
[39] The GSSort package, http://www.phy.anl.gov/gammasphere/doc/index.html, 2015.
[40] T. Yamazaki, Tables of coefficients for angular distribution of gamma rays from aligned nuclei, Nuclear Data Sheets. Section A **3**, 1 (1967).
[41] L. I. Govor, A. M. Demidov, and V. A. Kurkin, Study of transitions of 140ce in the reaction (n,n'γ)? Physics of Atomic Nuclei **56**, 1625 (1993).
[42] E. Browne, Calculated uncertainties of absolute γ-ray intensities and decay branching ratios derived from decay schemes, Nucl. Instrum. Methods Phys. Res. Sect. A **249**, 461 (1986).